LUPINE PUBLISHERS
Open Access

Archives of Organic and Inorganic Chemical Sciences

DOI: 10.32474/AOICS.2018.03.000171

ISSN: 2637-4609

Research Article

Spectroscopy and Dipole Moment of the Molecule $C_{13}H_{20}BeLi_2SeSi$ Via Quantum Chemistry using Ab Initio, Hartree-Fock Method in the Base Set CC-Pvtz and 6-311G**(3df, 3pd)

Ricardo Gobato[1]*, Marcia Regina Risso Gobato[2], Alireza Heidari[3] and Abhijit Mitra[4]

[1]*Laboratory of Biophysics and Molecular Modeling Genesis, State Secretariat for Education of Parana, Bela Vista do Paraiso, Parana, Brazil*

[2]*Seedling Growth Laboratory, Green Land Landscaping and Gardening, Bela Vista do Paraiso, Parana, Brazil*

[3]*Faculty of Chemistry, California South University, 14731 Comet St. Irvine, CA 92604, USA*

[4]*Department of Marine Science, University of Calcutta, West Bengal, India*

Received: September 03, 2018; **Published:** September 24, 2018

***Corresponding author:** Ricardo Gobato, Laboratory of Biophysics and Molecular Modeling Genesis, State Secretariat for Education of Parana, Bela Vista do Paraiso, Parana, Brazil

Abstract

The work characterizes the electric dipole moment and the infrared spectrum of the molecule $C_{13}H_{20}BeLi_2SeSi$. Calculations obtained in the ab initio RHF (Restrict Hartree-Fock) method, on the set of bases used indicate that the simulated molecule $C_{13}H_{20}BeLi_2SeSi$ features the structure polar-apolar-polar predominant. The set of bases used that have are CC-pVTZ and 6-311G** (3df, 3pd). In the CC-pVTZ base set, the charge density in relation to 6-311G** (3df, 3pd) is 50% lower. The length of the molecule $C_{13}H_{20}BeLi_2SeSi$ is of 15.799Å. The magnitude of the electric dipole moment || total obtained was p = 4.9771 Debye and p = 4.7936 Debye, perpendicular to the main axis of the molecule, for sets basis CC-pVTZ and 6-311**(3df, 3pd), respectively. The infrared spectra for absorbance and transmittance and their wavenumber (cm^{-1}) were obtained in the set of bases used. The infrared spectrum for Standard CC-pVTZ shows peaks in transmittance with Intensity (I), at wavenumber 1,125.44cm^{-1}, 1,940.70cm^{-1}, 2,094.82cm^{-1}, 2,178.43cm^{-1}, 2,613.99cm^{-1} and transmittance 433.399km/mol, 399.425km/mol, 361.825km/mol, 378.993km/mol, 433.774km/mol, respectively. While the infrared spectrum for Standard 6-311G** (3df,3pd), shows peaks in transmittance, at wavelengths 1,114.83cm^{-1}, 1,936.81cm^{-1}, 2,081.49cm^{-1}, 2,163.23 cm^{-1}, 2,595.24cm^{-1} and transmittance 434.556 km/mol, 394.430 km/mol, 345.287 km/mol, 375.381 km/mol, 409.232 km/mol, respectively. It presents "fingerprint" between the intervals (680cm^{-1} and 1,500 cm^{-1}) and (3,250cm^{-1} and 3,500cm^{-1}). The dipole moments CC-pTZV are 3.69% bigger than 6-311G (3df, 3pd). As the bio-inorganic molecule $C_{13}H_{20}BeLi_2SeSi$ is the basis for a new creation of a bio-membrane, later calculations that challenge the current concepts of biomembrane should advance to such a purpose.

Introduction

The work characterizes the electric dipole moment and the infrared spectrum of the molecule $C_{13}H_{20}BeLi_2SeSi$ [1]. Using a computational simulation using ab initio methods, RHF (Restrict Hartree-Fock), [2-9] set of basis CC-pVTZ [10-14] and 6-311G (3df, 3pd) [7,5-21]. Preliminary bibliographic studies did not reveal any works with characteristics studied here. There is an absence of a referential of the theme, finding only one work in [1]. To construct such a molecule, which was called a seed molecule, quantum chemistry was used by ab initio methods [2,3,15]. The equipment used was of the Biophysics laboratory built specifically for this task. The results were satisfactory. The ab initio calculations, by RHF [2-9] in the CC-pVTZ [10-14] and 6-311G (3df, 3pd) [7,15-21], sets basis was shown to be stable by changing its covalent cyclic chain linkages, which was expected. The set of basis used was that of Ahlrichs and coworkers the TZVP keywords refer to the initial formations of the split valence and triple zeta basis sets from this group [22,23]. The structure of the $C_{13}H_{20}BeLi_2SeSi$ is a Bio-inorganic seed molecule for a biomembrane genesis that defies the current concepts of a protective mantle structure of a cell such as biomenbrane to date is promising, challenging. Leaving to the Biochemists their experimental synthesis. The quantum calculations must continue to obtain the structure of the bio-inorganic biomenbrane. The following calculations, which are the computational simulation via Mm+, QM/MM, should indicate what type of structure should form. Structures of a liquid crystal such as a new membrane may occur, micelles [1,24-62].

Methods

Hartree-Fock Methods

Hartree-Fock theory is one the simplest approximate theories for solving the many-body Hamiltonian [2-9]. The full Hartree-Fock equations are given by

$$\epsilon_i \varphi_i(r) = (-\frac{1}{2}\nabla^2 + V_{ion}(r))\varphi_i(r) + \sum_i \int dr' \frac{|\varphi_j(r')|^2}{|r-r'|}\varphi_i(r) - \sum_j \delta_{\sigma_i\sigma_j} \int dr' \frac{\varphi^*_j(r')\varphi_i(r')}{|r-r'|}\varphi_j(r). \quad (1)$$

The vast literature associated with these methods suggests that the following is a plausible hierarchy:

$$HF \ll MP2 < CISD < CCSD < CCSD(T) < FCI \quad (2)$$

The extremes of 'best', FCI, and 'worst', HF, are irrefutable, but the intermediate methods are less clear and depend on the type of chemical problem being addressed. [63,64] The use of HF in the case of FCI was due to the computational cost [1, 24-62].

Hardware and Software

For Calculations A Computer Models was Used: Intel® Core™ i3-3220 CPU@3.3 GHz x 4 processors [65], Memory DDR3 4 GB, HD SATA WDC WD7500 AZEK-00RKKA0 750.1 GB and DVD-RAM SATA GH24NS9 ATAPI, Graphics Intel® Ivy Bridge [66]. The ab initio calculations have been performed to study the equilibrium configuration of $C_{13}H_{20}BeLi_2SeSi$ molecule using the GAMESS [15,20]. The set of programs Gauss View 5.0.8 [67], Mercury 3.8 [68], Avogadro [69,70] are the advanced semantic chemical editor, visualization, and analysis platform and GAMESS [15,20] is a computational chemistry software program and stands for General Atomic and Molecular Electronic Structure System [15,20] set of programs. For calculations of computational dynamics, the Ubuntu Linux version 16.10 system was used [71].

Result

(Figures 1-5) and (Tables 1-3).

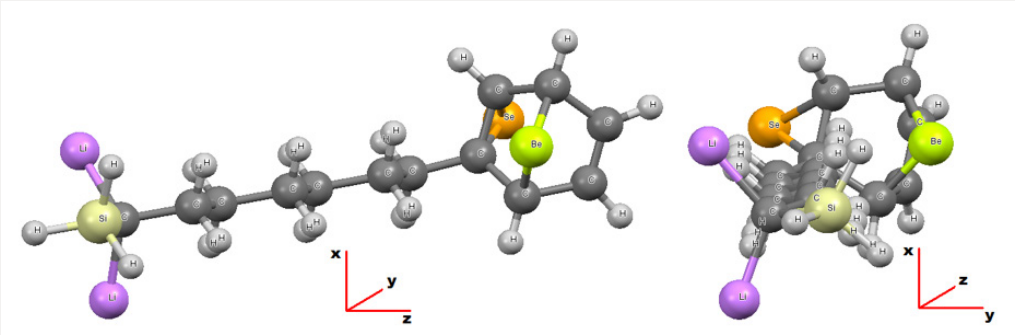

Figure 1: Representation of the molecular structure of C13H20BeLi2SeSi, obtained through computer via ab initio calculation method RHF [2-9], CC-pVTZ [10-14] sets basis obtained using computer programs GAMESS [15,20]. Images obtained in the software Mercury 3.8 [68]. Represented in bluish gray color the atom of silicon, in the purple color lithium, in the lemon yellow color beryllium, in the orange the selenium, in dark gray color carbon and in light gray color hydrogen. The image from left to right has a 90 degree rotation in the YZ plane, anti-clockwise.

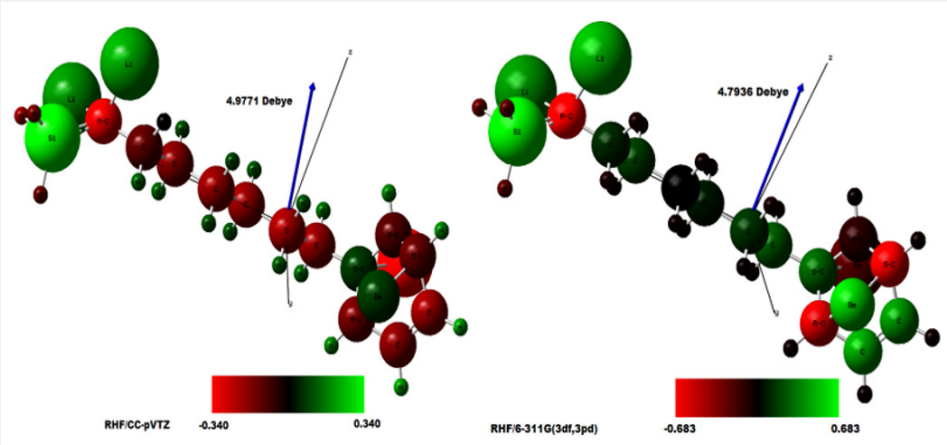

Figure 2: Molecule bio-inorganic $C_{13}H_{20}BeLi_2SeSi$ after dynamics obtained through computer via ab initio calculation method RHF [2-9] in sets of basis obtained using computer software GAMESS [15,20]. The length of the molecule $C^{13}H_{20}BeLi_2SeSi$ obtained in the base CC-pVTZ [10-14] is of 15.799Å. Represented in green color the positive charge, passing through the absence of color - black - zero charge, for the positive charge red color. A Δδ = 0.680 a.u. of CC-pVTZ [10-14] and Δδ = 1.366 a.u. of 6-311**(3df,3pd) [7,15-21], were the elemental charge e (e = ±1,607 x 10-19 C). Images obtained in the software Gaussview, Version 5, 2009 [67].

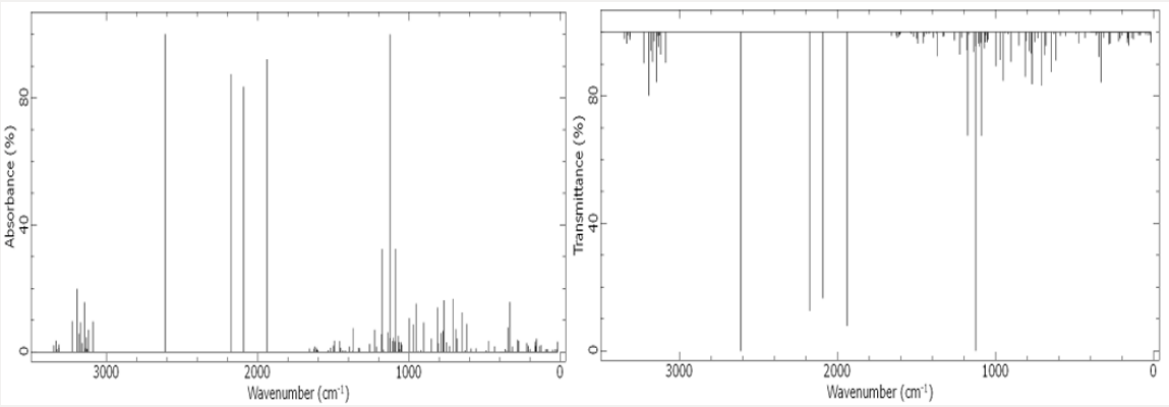

Figure 3: Characteristic infrared spectrum in absorbance and transmittance obtained using the ab initio HF method for the RHF [5-6,27-32] in sets of basis CC-pVTZ [10-14] obtained using computer software GAMESS [15,20]. Image created by Avogadro software [69,70].

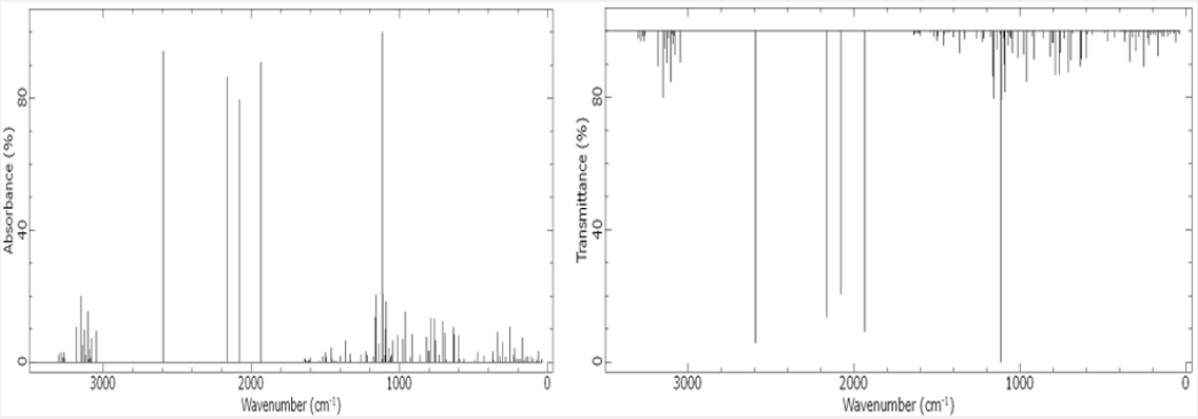

Figure 4: Characteristic infrared spectrum in absorbance and transmittance obtained using the ab initio HF method for the RHF [2-9] in sets of basis RHF/6-311G**(3df,3pd) [7,15-21] obtained using computer software GAMESS [15,20]. Image created by Avogadro software [69,70].

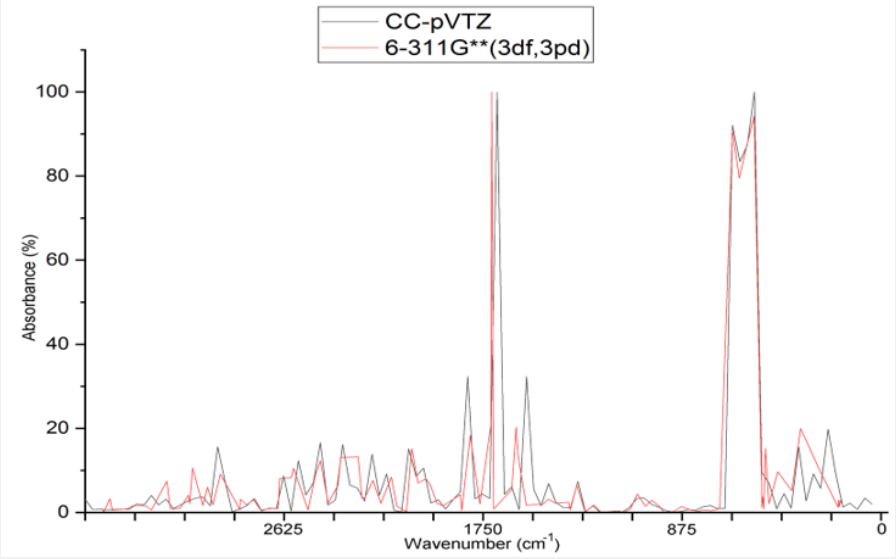

Figure 5: Infrared spectrum obtained using the ab initio for the RHF [2-9] method, in sets of basis RHF/CC-pVTZ [10-14] in black color and 6-311G**(3df, 3pd) [7,15-21] in red color, obtained using computer software GAMESS [15,20]. Graphic edited in origin software, for comparison of the spectra obtained in the set of bases used [72].

Table 1: Table containing the dipole moments of the $C_{13}H_{20}BeLi_2SeSi$ molecule via ab initio methods. [1,24-62].

Methods/Base	Dipole Msssoment (Debye)				Charge (a. u.)	
	X	Y	Z	Total	δ±	Δδ
RHF/CC-pVTZ [10-14]	1.0338	1.616	4.5925	4.9771	0.34	0.68
RHF/6-311G(3df,3pd)[7,15-21]	0.8366	1.0963	4.591	4.7936	0.683	1.366

Selects Stuttgart potentials for Z > 2. MC-311G is a synonym for 6-311G [7]. The elemental charge e (e = ±1,607 x 10^{-19} C) [1,24-62].

Table 2: Table containing the frequency (cm^{-1}) for Intensity (km/mol) of the $C_{13}H_{20}BeLi_2SeSi$ molecule via ab initio methods, set base RHF/CC-pVTZ [10-14] for the infrared spectrum.

υ(cm^{-1})	I(km/mol)	υ(cm^{-1})	I(km/mol)	υ(cm^{-1})	I(km/mol)	υ(cm^{-1})	I(km/mol)	υ(cm^{-1})	I(km/mol)
18.3102	3.12029	433.777	1.66974	953.826	15.1296	1335.63	1.20528	1940.7	92.0814
21.8078	0.71641	474.621	3.33766	972.128	8.56993	1368.61	7.38902	2094.82	83.4134
33.8524	0.774	490.566	0.397	998.024	10.538	1377.96	0.19303	2178.43	87.3712
50.7492	0.6301	558.722	1.05878	1048.59	2.26512	1394.93	1.58394	2613.39	100
84.5077	0.72158	590.954	1.00084	1055.46	3.03114	1418.8	0.14913	3089.67	9.49051
86.629	0.81646	617.372	8.74975	1064.35	0.81462	1424.6	0.17433	3120.01	6.88461
97.8753	0.74488	630.277	0.38728	1067.42	3.02414	1436.44	0.31307	3128.33	0.89217
126.23	2.0401	647.261	12.3518	1071.03	4.96342	1441.47	0.07686	3135.24	4.50814
137.242	1.7991	682.22	4.12012	1089.2	32.3829	1452.56	1.20736	3138.75	1.03164
157.219	4.05892	689.18	7.0704	1094.53	3.21532	1458.87	3.30915	3146.5	15.5662
162.276	1.7985	707.797	16.6292	1101.9	4.3657	1493.82	3.44459	3162.12	2.74526
166.155	3.18327	732.622	1.7602	1110.7	3.3637	1500.51	1.9095	3173.18	9.21057
198.816	0.89883	750.917	2.93531	1125.44	99.9136	1519.22	1.26635	3184.08	5.71116
212.187	1.86318	769.859	16.1805	1127.23	4.2888	1535.04	0.44678	3194.99	19.7912
221.476	2.72144	776.501	6.54948	1141	6.0932	1539.78	0.07426	3227.87	9.59669
275.674	3.41994	787.004	5.83286	1168.18	0.62429	1602.19	0.25765	3316.21	1.26114
282.521	3.70827	807.718	2.6583	1178.46	32.3097	1605.82	0.68637	3317.19	2.26056
317.555	1.59558	813.453	13.892	1181.38	5.50813	1609.5	0.5261	3327.04	0.77109
334.037	15.6202	852.383	4.08084	1215.09	1.56665	1614.85	1.3661	3334.54	3.46058
345.691	7.59721	904.189	9.17924	1227.79	6.88714	1623.77	1.61794	3350.07	1.98841
355.229	0.19418	922.235	0.47511	1261.09	2.41179	1632.4	0.92053	-	-
364.062	0.83481	939.486	0.16712	1327.9	1.12109	1658.79	0.99144	-	-

Table 3: Table containing the frequency (cm^{-1}) for Intensity (km/mol) of the $C_{13}H_{20}BeLi_2SeSi$ molecule via ab initio methods, set base RHF/6-311G**(3df,3pd) [7,15-21] for the infrared spectrum.

υ(cm^{-1})	I(km/mol)	υ(cm^{-1})	I(km/mol)	υ(cm^{-1})	I(km/mol)	υ(cm^{-1})	I(km/mol)	υ(cm^{-1})	I(km/mol)
39.369	0.88442	431.663	1.86731	961.239	15.1899	1335.2	0.61688	1936.81	90.7662
42.923	0.17054	471.044	3.035	978.668	6.97516	1363.74	6.53782	2081.49	79.4573
62.8276	3.28814	488.826	0.53052	1014.2	8.05159	1377.72	0.1169	2163.23	86.3825
72.7607	0.56446	565.761	1.00387	1046.06	6.55719	1400.12	1.82204	2595.24	94.1724
95.4188	0.93953	596.729	0.9032	1054.41	2.19171	1419.33	0.02732	3047.17	9.41218
110.899	1.5728	601.67	8.03745	1061.36	1.55943	1427.28	0.22738	3078.87	7.12474
134.966	1.59724	630.486	8.2894	1071.3	4.21379	1439.56	0.32592	3085.2	1.20834
143.076	1.53324	636.16	10.5322	1074.67	0.45713	1444.66	0.01565	3093.54	3.80278
157.293	0.56626	684.438	0.59237	1091.08	18.3426	1453.38	0.89434	3097.22	0.83218
169.689	7.45772	694.387	8.79184	1094.82	9.94311	1461.7	4.3766	3104.6	15.3096
183.992	1.0276	707.931	12.3189	1099.32	2.01902	1495.15	1.47712	3118.77	2.09616
196.879	0.82397	732.994	2.16414	1112.97	20.6379	1500.48	2.89203	3129.36	9.65626

211.297	1.02116	758.028	6.54359	1114.83	100	1519.04	1.63496	3139.28	5.15606
223.037	4.09832	765.144	13.0978	1118.45	0.82424	1530	0.02538	3150.53	19.9936
232.038	2.0543	789.539	13.2657	1141.23	5.42491	1542.72	0.26491	3181.23	10.5582
254.819	10.5952	800.107	3.41912	1157.39	20.3207	1602.47	1.41178	3261.85	1.17952
282.795	1.64299	807.546	3.44432	1164.58	13.5674	1607.45	0.51568	3265.57	2.95239
304.708	6.03544	818.874	7.61634	1178.37	1.67813	1612.6	0.31253	3275.09	1.44561
323.719	1.83394	862.268	2.15917	1219.22	2.10679	1614.24	0.64217	3284.35	2.97161
338.676	9.13437	915.264	8.40579	1227.29	3.20311	1624.64	0.43792	3301.01	2.20326
366.646	0.6358	928.717	1.5306	1259.71	2.2045	1635.27	0.87439	-	-
369.57	3.1317	949.146	0.13393	1333.44	2.44035	1639.76	1.06541	-	-

Discussion

The Figure 1 shows the final stable structure of the bio-inorganic $C_{13}H_{20}BeLi_2SeSi$ molecule obtained by an *ab initio* calculation with the method RHF (Restrict Hatrree-Fock), in sets of bases such as: 6-311G**(3df,3pd) and CC-pVTZ. As an example of analysis the set of bases CC-pVTV, with the charge distribution (Δδ) through it, whose charge variation is Δδ = 0.680 a.u. of elemental charge. In green color the intensity of positive charge displacement. In red color the negative charge displacement intensity. Variable, therefore, of δ^- = 0.340 a.u. negative charge, passing through the absence of charge displacement, represented in the absence of black - for the green color of δ^+ = 0.340 a.u. positive charge. The magnitude of the electric dipole moment || total obtained was p =4.9771 Debye, perpendicular to the main axis of the molecule, for sets basis CC-pVTZ. By the distribution of charge through the bio-inorganic molecule it is clear that the molecule has a polar-apolar-polar structure, Figure 2 and Table 1. An analysis of the individual charge value of each atom of the molecule could be made, but here it was presented only according to Figure 2, due to the objective being to determine the polar-apolar-polar, the polar characteristic of the molecule, whose moment of dipole is practically perpendicular to the central axis of the molecule. In Figure 2 the dipole moment is visualized 6-311G**(3df,3pd) and CC-pVTZ in base sets, being represented by an arrow in dark blue color, with their respective values in Debye. This also presents the orientation axes x, y and z and the distribution of electric charges through the molecule.

In the set of bases used the CC-pTZV and 6-311**(3df, 3pd) present the same characteristic for the distribution of charges to the polar end with Carbon atom (negative charge) bound to the $-SiH_3$ radical and the two Lithium atoms. It is seen that Δδ =0.680 a.u. of CC-pTZV and Δδ =1.366 a.u. of 6-311 (3df, 3pd), this latter has a twice greater Δδ, Figure 2, although the dipole moments CC-pTZV are 3.69% larger, (Table 1). The main chain (backbone of the molecule) for the CC-pTZV base set has a small negative charge displacement for the Carbon atoms from the Hydrogen atoms attached to them. Therefore, with positive charge the Hydrogen atoms connected to the Carbon of the central chain. For the set of bases 6-311**(3df, 3pd) the carbon atoms of the main chain are presented with very small distribution of negative charge, coming from the Hydrogen linked to these neutrals, Figure 2. At the other polar end for the base set 6-311**(3df, 3pd) the cyclic chain shows the characteristics as the Beryllium atom with strong charge displacement positive, these charges shift to the Carbon atoms attached to it, Figure 2. The cyclic chain with a strong negative charge, displaced from the Beryllium atom. The two carbon atoms bonded in double bonds, present a slight positive charge, with their neutral Hydrogen, Figure 2. The Selenium atom connected to two Carbon atoms of the cyclic chain presents a slight negative charge, originating from the Carbon atom connected to the main chain with a slight positive charge, and the other Carbon atom connected to the cyclic chain presents a neutral charge, Figure 2. The magnitude of the electric dipole moment || total obtained was *p = 4.7936* Debye for 6-311**(3df, 3pd), (Table 1). Figures 3 & 4 represent the normalized infrared spectrum for the base set RHF / 6-311G ** (3df, 3pd) and CC-pVTZ for Absorbance and Transmittance. Figures 5 represent the normalized infrared spectrum for the base set RHF/6-311G** (3df, 3pd and CC-pVTZ for absorbance, making a comparison between the two sets of base. The infrared spectrum for Standard RHF/CC-pVTZ shows peaks in transmittance, at wavelengths 1,125.44cm^{-1}, 1,940.70cm^{-1}, 2,094.82cm^{-1}, 2,178.43cm^{-1}, 2,613.99cm^{-1} and transmittance 433.399km/mol, 399.425km/mol, 361.825km/mol, 378.993km/mol, 433.774km/mol, respectively, Figure 3 and Table 2. The infrared spectrum for Standard RHF/6-311G**(3df,3pd) shows peaks in transmittance, at wavelengths 1,114.83cm^{-1}, 1,936.81cm^{-1}, 2,081.49cm^{-1}, 2,163.23 cm^{-1}, 2,595.24cm^{-1} and transmittance 434.556km/mol, 394.430 km/mol, 345.287 km/mol, 375.381 km/mol, 409.232 km/mol, respectively, Figure 4 and Table 3. It presents "fingerprint" between the intervals (680cm^{-1} and 1,500cm^{-1}) and (3,250cm^{-1} and 3,500cm^{-1}), Figures 3-5.

Conclusion

Calculations obtained in the ab initio RHF method, on the set of bases used, indicate that the simulated molecule, $C_{13}H_{20}BeLi_2SeSi$, is acceptable by quantum chemistry. Its structure has polarity at its ends, having the characteristic polar-apolar-polar. The 6-311G (3df, 3pd) set of basis exhibits the characteristic of the central chain, with a small density of negative charges, near the ends of the Carbons of this. In the CC-pVTZ base set, the charge density in relation to 6-311G (3df, 3pd) is 50% lower. It is characterized infrared spectrum of the molecule $C_{13}H_{20}BeLi_2SeSi$, for absorbance and transmittance, in Hartree method in the set of bases CC-pVTZ

and 6-311G (3df, 3pd). The infrared spectrum for Standard RHF/CC-pVTZ shows peaks in transmittance, at wavelengths 1,125.44cm^{-1}, 1,940.70cm^{-1}, 2,094.82cm^{-1}, 2,178.43cm^{-1}, 2,613.99cm^{-1} and transmittance 433.399 km/mol, 399.425km/mol, 361.825km/mol, 378.993km/mol, 433.774km/mol, respectively. The infrared spectrum for Standard RHF/6-311G**(3df,3pd) [7,30,60,71,72] shows peaks in transmittance, at wavelengths 1,114.83cm^{-1}, 1,936.81cm^{-1}, 2,081.49cm^{-1}, 2,163.23cm^{-1}, 2,595.24cm^{-1} and transmittance 434.556km/mol, 394.430km/mol, 345.287km/mol, 375.381km/mol, 409.232km/mol, respectively. It presents "fingerprint" between the intervals (680cm^{-1} and 1,500cm^{-1}) and (3,250cm^{-1} and 3,500cm^{-1}). The dipole moments CC-pTZV are 3.69% bigger than 6-311G (3df, 3pd). As the bio-inorganic molecule $C_{13}H_{20}BeLi_2SeSi$ is the basis for a new creation of a bio-membrane, later calculations that challenge the current concepts of biomembrane should advance to such a purpose.

Acknowledgement

To the doctors: Prof. Ph.D. Tolga Yarman, Okan University, Akfirat, Istanbul, Turkey & Savronik, Organize Sanayi Bolgesi, Eskisehir, Turkey, and Prof. Ph.D. Ozan Yarman, Istanbul University, Rihtim Nr:1, 81300 Kadikoy, Istanbul, Turkey, for their valuable contributions to the work.

References

1. Gobato R, Heidari A, Mitra A (2018) The Creation of C13H20BeLi2SeSi. The Proposal of a Bio-Inorganic Molecule, Using Ab Initio Methods for The Genesis of a Nano Membrane. Arc Org Inorg Chem Sci 3(4): 112-115.
2. Levine IN (2003) Quantum Chemistry. Pearson Education (Singapore) (5th edn.); Delhi, India.
3. Szabo A, Ostlund NS (1989) Modern Quantum Chemistry. Dover Publications, New York, USA.
4. Ohno K, Esfarjani K, Kawazoe Y (1999) Computational Material Science. Springer-Verlag, Berlin.
5. Wolfram K, Hothausen MC (2001) Introduction to DFT for Chemists (2nd edn.); John Wiley & Sons, New York, USA.
6. Hohenberg P, Kohn W (1964) Inhomogeneous electron gas. Phys Rev 136: B864-B871.
7. Kohn W, Sham LJ (1965) Self-consistent equations including exchange and correlation effects. Phys Rev 140: A1133.
8. Thijssen JM (2001) Computational Physics. Cambridge University Press, Cambridge, USA.
9. Perdew M, Ernzerhof, Burke K (1996) Rationale for mixing exact exchange with density functional approximations. J Chem Phys 105(22): 9982-9985.
10. Dunning TH (1983) Gaussian basis sets for use in correlated molecular calculations, The atoms boron through neon and hydrogen. J Chem Phys 90: 1007-1023.
11. Kendall RA, Dunning TH, Harrison RJ (1992) Electron affinities of the first-row atoms revisited. Systematic basis sets and wave function. J Chem Phys 96: 6796-67806.
12. Woon DE, Dunning (1993) Gaussian-basis sets for use in correlated molecular calculations. The atoms aluminum through argon. J Chem Phys 98: 1358-1371.
13. Peterson KA, Woon DE, Dunning TH (1994) Benchmark calculations with correlated molecular wave functions. The classical barrier height of the H+H2 -¿ H2+H reaction. J Chem Phys 100: 7410-7415.
14. Wilson AK, van Mourik T, Dunning TH (1996) Gaussian basis sets for use in Correlated Molecular Calculations. Sextuple zeta correlation consistent basis sets for boron through neon. J Mol Struct (Theochem) 388: 339-349.
15. Gordon MS (1993) General atomic and molecular electronic structure system (GAMESS). J Comput Chem 14: 1347-1363.
16. Polak E (1971) Computational Methods in Optimization. Elsevier, New York, USA.
17. Dunning TH, Hay PJ (1997) Modern Theoretical Chemistry. Plenum, New York, USA.
18. Eliav E (2013) Elementary introduction to Molecular Mechanics and Dynamics.
19. Hehre WJ (2003) A Guide to Molecular Mechanics and Quantum Chemical Calculations. Wavefunction, Inc, Irvine, CA.
20. Gordon MS, Schmidt MW (2005) Advances in electronic structure theory: GAMESS a decade later. Theory and Applications of Computational Chemistry: The first forty years pp. 1167-1189.
21. Amsterdam RG Parr W, Yang (1989) Density Functional Theory.
22. Schaefer A, Huber C, Ahlrichs R (1992) Fully optimized contracted Gaussian-basis sets for atoms Li to Kr. J Chem Phys 97: 2571-2577.
23. Schaefer A, Huber C, Ahlrichs R (1994) Fully optimized contracted Gaussian-basis sets of triple zeta valence quality for atoms Li to Kr. J Chem Phys 100: 5829-5835.
24. Gobato R, Fedrigo DFG, Gobato A (2014) Inorganic arrangement crystal beryllium, lithium, selenium and silicon. In XIX Semana da Física. Simpósio Comemorativo dos 40 anos do Curso de Física da Universidade Estadual de Londrina. BrazilUniversidade Estadual de Londrina (UEL).
25. Gobato R (2018) Benzocaína, um estudo computacional. Master's thesis, Universidade Estadual de Londrina.
26. Gobato R (2017) Study of the molecular geometry of Caramboxin toxin found in star flower (*Averrhoa carambola* L.). Parana J Sci Edu 3(1): 1-9.
27. Gobato R, Fedrigo DFG, Gobato A (2015) Molecular electrostatic potential of the main monoterpenoids compounds found in oil Lemon Tahiti - (Citrus Latifolia Var Tahiti). Parana J Sci Edu 1(1): 1-10.
28. Gobato R, Fedrigo DFG, Gobato A (2015) Allocryptopine, Berberine, Chelerythrine, Copsitine, Dihydrosanguinarine, Protopine and Sanguinarine. Molecular geometry of the main alkaloids found in the seeds of Argemone Mexicana Linn. Parana J Sci Edu 1(2): 7-16.
29. Gobato R, Heidari A (2018) Infrared Spectrum and Sites of Action of Sanguinarine by Molecular Mechanics and ab initio Methods. International Journal of Atmospheric and Oceanic Sciences 2(1): 1-9.
30. Gobato R, Fedrigo DFG, Gobato A (2015) Molecular geometry of alkaloids present in seeds of mexican prickly poppy. Cornell University Library. Quantitative Biology arXiv: 1507.05042.
31. Gobato R, Fedrigo DFG, Gobato A (2018) Study of the molecular electrostatic potential of D-Pinitol an active hypoglycemic principle found in Spring flower Three Marys (*Bougainvillea* species) in the Mm+ method. Parana J Sci Educ 2(4): 1-9.
32. Gobato R, Fedrigo DFG, Gobato A (2015) Avro: key component of Lockheed X-35. Parana J Sci Educ 1(2): 1-6.
33. Gobato R, Fedrigo DFG, Gobato A (2016) LOT-G3: Plasma Lamp, Ozonator and CW Transmitter. Cienciae Natura 38(1): 453.

34. Gobato R (2016) Matter and energy in a non-relativistic approach amongst the mustard seed and the faith. A metaphysical conclusion. Parana J Sci Educ 2(3): 1-14.

35. Gobato R, Fedrigo DFG, Gobato A (2016) Harnessing the energy of ocean surface waves by Pelamis System. Parana J Sci Educ 2(2): 1-15.

36. Gobato R, Fedrigo DFG, Gobato A (2016) Mathematics for input space probes in the atmosphere of Gliese 581d. Parana J Sci Educ 2(5): 6-13.

37. Gobato R, Fedrigo DFG, Gobato A (2006) Study of tornadoes that have reached the state of Parana. Parana J Sci Educ 2(1): 1-27.

38. Gobato R, Simões F (2017) Alternative Method of RGB Channel Spectroscopy Using a CCD Reader. Ciencia e Natura 39(2).

39. Gobato R, Heidari A (2017) Calculations Using Quantum Chemistry for Inorganic Molecule Simulation BeLi2SeSi. Science Journal of Analytical Chemistry 5(5): 76-85.

40. Gobato MRR, Gobato A, Heidari (2018) Planting of Jaboticaba Trees for Landscape Repair of Degraded Area. Landscape Architecture and Regional Planning 3(1): 1-9.

41. Gobato R (2012) The Liotropic Indicatrix 114: 62.

42. Gobato R, Heidari A (2018) Calculations Using Quantum Chemistry for Inorganic Molecule Simulation BeLi2SeSi. Science Journal of Analytical Chemistry 5(6): 76-85.

43. Gobato MRR, Gobato R, Heidari A (2018) Planting of Jaboticaba Trees for Landscape Repair of Degraded Area. Landscape Architecture and Regional Planning 3(1): 1-9.

44. Gobato MRR, Gobato R, Heidari A (2018) Infrared Spectrum and Sites of Action of Sanguinarine by Molecular Mechanics and ab initio Methods. International Journal of Atmospheric and Oceanic Sciences 2(1): 1-9.

45. Gobato MRR, Gobato R, Heidari A (2018) Molecular Mechanics and Quantum Chemical Study on Sites of Action of Sanguinarine Using Vibrational Spectroscopy Based on Molecular Mechanics and Quantum Chemical Calculations. Malaysian Journal of Chemistry 20(1): 1-23.

46. Gobato MRR, Gobato R, Heidari A (2018) A Novel Approach to Reduce Toxicities and to Improve Bioavailabilities of DNA/RNA of Human Cancer Cells-Containing Cocaine (Coke), Lysergide (Lysergic Acid Diethyl Amide or LSD), Δ^9-Tetrahydrocannabinol (THC) [(-)-trans-Δ^9-Tetrahydrocannabinol], Theobromine (Xantheose), Caffeine, Aspartame (APM) (NutraSweet) and Zidovudine (ZDV) [Azidothymidine (AZT)] as Anti-Cancer Nano Drugs by Coassembly of Dual Anti-Cancer Nano Drugs to Inhibit DNA/RNA of Human Cancer Cells Drug Resistance. Parana Journal of Science and Education 4(6): 1-17.

47. Gobato R, Heidari A (2018) Ultraviolet Photoelectron Spectroscopy (UPS) and Ultraviolet-Visible (UV-Vis) Spectroscopy Comparative Study on Malignant and Benign Human Cancer Cells and Tissues with the Passage of Time under Synchrotron Radiation. Parana Journal of Science and Education 4(6): 18-33.

48. Gobato R, Heidari A (2018) Using the Quantum Chemistry for Genesis of a Nano Biomembrane with a Combination of the Elements Be, Li, Se, Si, C and H. J Nanomed Res 7(4): 241-252.

49. Gobato R, Heidari A (2014) Inorganic arrangement crystal beryllium, lithium, selenium and silicon. Universidade Estadual de Londrina (UEL), arXiv: 1508-00175.

50. Gobato R (2017) Study of the molecular geometry of Caramboxin toxin found in star flower (*Averrhoa carambola* L.). Parana J Sci Educ 3(1): 1-9.

51. Gobato R, Gobato A, Fedrigo DFG (2015) Molecular electrostatic potential of the main monoterpenoids compounds found in oil Lemon Tahiti - (Citrus Latifolia Var Tahiti). Parana J Sci Educ 1(1): 1-10.

52. Gobato R, Fedrigo DFG, Gobato A (2015) Allocryptopine, Berberine, Chelerythrine, Copsitine, Dihydrosanguinarine, Protopine and Sanguinarine. Molecular geometry of the main alkaloids found in the seeds of Argemone Mexicana Linn. Parana J Sci Educ 1(2):7-16.

53. Gobato R, Heidari A (2018) Infrared Spectrum and Sites of Action of Sanguinarine by Molecular Mechanics and ab initio Methods. International Journal of Atmospheric and Oceanic Sciences 2(1): 1-9.

54. Gobato R, Fedrigo DFG, Gobato A (2015) Molecular geometry of alkaloids present in seeds of mexican prickly poppy. Quantitative Biology arXiv: 1507.05042.

55. Gobato R, Fedrigo DFG, Gobato A (2016) Study of the molecular electrostatic potential of D-Pinitol an active hypoglycemic principle found in Spring flower Three Marys (*Bougainvillea* species) in the Mm+ method. Parana J Sci Educ 2(4): 1-9.

56. Gobato R, Fedrigo DFG, Gobato A (2015) Avro: key component of Lockheed X-35. Parana J Sci Educ 1(2): 1-6.

57. Agarwal SK, Roy S, Pramanick P, Mitra P, Gobato R, et al. (2018) Marsilea quadrifolia: A floral species with unique medicinal properties. Parana J Sci Educ 4(5): 15-20.

58. Mitra A, Zaman S, Gobato R (2018) Indian Sundarban Mangroves: A potential Carbon Scrubbing System. Parana J Sci Educ 4(4): 7-29.

59. Yarman O, Gobato R, Yarman T, Arik M (2018) A new Physical constant from the ratio of the reciprocal of the "Rydberg constant" to the Planck length. Parana J Sci Educ 4(3): 42-51.

60. Gobato R, Simões F (2017) Alternative Method of Spectroscopy of Alkali Metal RGB. Modern Chemistry 5(4): 70-74.

61. Fedrigo DFG, Gobato R, Gobato A (2015) Avrocar: a real flying saucer. Cornell University Library arXiv: 1507.

62. Fedrigo DFG, Gobato R, Gobato A (2012) Micellar shape anisotropy and optical indicatrix in reentrant isotropic-nematic phase transitions. The Journal of Chemical Physics 137: 204905.

63. McDouall JJW (2013) Computational Quantum Chemistry. Molecular Structure and Properties in Silico. Royal Society of Chemistry p. 1-62.

64. Weigend F, Ahlrichs R (2005) Balanced basis sets of split valence, triple zeta valence and quadruple zeta valence quality for H to Rn: Design and assessment of accuracy. Phys Chem Chem Phys 7(8): 3297-3298.

65. Creative Commons (CC BY 4.0) https://creativecommons.org/licenses/by/4.0/. List of Intel Core i3 microprocessors. https://en.wikipedia.org/wiki/List_of_Intel_Core_i3_microprocessors.

66. Ivy Bridge.

67. Dennington R, Keith T, Millam J, Gaussview (2009) Version 5.

68. The Cambridge Crystallographic Data Centre (CCDC) Mercury - crystal structure visualisation, exploration and analysis made easy. Mercury 3.1 Development (Build RC5). The Cambridge Crystallographic Data Centre.

69. Avogadro: an open-source molecular builder and visualization tool. Version 1.1.1.

70. Marcus D, Hanwell DE, Curtis DC, Lonie TV, Zurek E, et al. (2012) Avogadro: An advanced semantic chemical editor, visualization, and analysis platform. J Cheminform 4(1): 17.

71. Creative Commons, (CC BY 4.0), https://creativecommons.org/licenses/by/4.0/. Ubuntu (operating system). https://en.wikipedia.org/wiki/Ubuntu_(operating_system).

72. Origin Lab (2018) Evaluation Licence, Graphing & Analysis, ©OriginLab Corporation.

DOI: 10.32474/AOICS.2018.03.000171